

Linear elasticity of polymer gels in terms of negative energy elasticity

Naoyuki Sakumichi,^{1,*} Yuki Yoshikawa,¹ and Takamasa Sakai^{1,†}

¹*Department of Bioengineering, Graduate School of Engineering,
The University of Tokyo, 7-3-1 Hongo, Bunkyo-ku, Tokyo, Japan.*

(Dated: December 24, 2024)

We recently found that the energy contribution to the linear elasticity of polymer gels in the as-prepared state can be a significant negative value; the shear modulus is not proportional to the absolute temperature [Yoshikawa Y et al., Phys. Rev. X **11**, 011045 (2021)]. Our finding challenges the conventional notion that the polymer-gel elasticity is mainly determined by entropy contribution. Existing molecular models of classical rubber elasticity theories, including the affine, phantom, or junction affine network model, cannot be used to estimate the structural parameters of polymer gels. In this focus review, we summarize the experimental studies on the linear elasticity of polymer gels in the as-prepared state using tetra-arm poly(ethylene glycol) (PEG) hydrogels with a homogenous polymer network. We also provide a unified formula for the linear elasticity of polymer gels with various network topologies and densities. Using the unified formula, we resolve the past experimental results that seem to be inconsistent with each other. Finally, we mention that there are still fundamental unresolved problems with the linear elasticity of polymer gels.

I. INTRODUCTION

Polymer gels are widely used in food products such as yogurt, tofu, and jelly [1–3] and in biomaterials such as anti-adhesion agents, hemostatic agents, and soft contact lenses [4–6]. For these applications, it is important to control the softness of polymer gels. For example, soft polymer gels are used in artificial vitreous substitutes and food for dysphagia, and hard polymer gels in hemostatic agents and artificial cartilages. By optimizing the polymer gel softness for its intended use, quality of life (QOL) can be improved in various situations.

Despite the importance of controlling the softness, it is an open question how the softness of a polymer gel is determined by its microscopic network structure. The elasticity of a polymer gel, which is regarded as rubber containing a large amount of solvent, has been conventionally analyzed and predicted based on classical rubber elasticity theories, such as the affine [7], phantom [8], and junction affine network models [9]. However, it is difficult to verify the applicability of these microscopic models to macroscopic properties of polymer gels because the conventional polymer gels inherently have inhomogeneous network structures [10]. Thus, the determination of the appropriate microscopic model describing polymer-gel elasticity remains to be achieved [11, 12].

In recent years, we overcame the difficulty of inhomogeneity by developing a tetra-arm poly(ethylene glycol) (PEG) hydrogel (tetra gel) [13] with a homogeneous network structure [14] (Fig. 1a). In the tetra gel, we can

independently and systematically control the structure of the polymer network, as shown in Fig. 1b. Using tetra gels, we have studied the linear elasticity of polymer gels in the as-prepared state by various experimental techniques [13, 15–17].

Although we analyzed our experiments using existing models of the classical rubber elasticity theories until recently, we observed inconsistencies with respect to the interpretations of experimental results as described in Sec. II. A very recent discovery revealed that polymer gels have “negative energy elasticity” [18], namely a significant negative internal energy contribution to the shear modulus originating from the solvent. This is not considered in the classical rubber elasticity theories, which assume that the elastic modulus is mainly determined from entropy contribution. Because the internal energy contribution is significant and negative, the (hidden) entropy contribution is large compared to the total modulus. Our discovery challenges the conventional notion that elasticity of polymer gel can be understood by the classical rubber elasticity theories.

In this focus review, we describe how past experimental results on the linear elasticity of polymer gels can be successfully explained by the existence of negative energy elasticity. This focus review is organized as follows. First, we briefly review the experimental study on the linear elasticity of polymer gels. Second, we present the current state-of-the-art of unified formula for the linear elasticity of polymer gels with various network topologies and densities. Third, using this formula, we re-examine the past experimental results. Finally, we present the summary and outlook of these investigations.

* sakumichi@tetrapod.t.u-tokyo.ac.jp

† sakai@tetrapod.t.u-tokyo.ac.jp

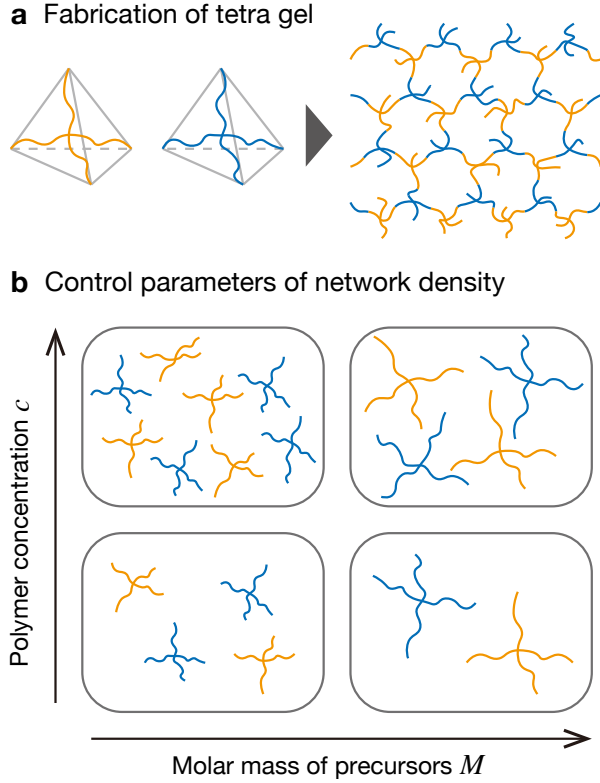


FIG. 1. **a** Tetra gel synthesized by AB-type cross-end coupling of two kinds of precursors of equal size in a water solvent. These precursors are tetra-arm poly(ethylene glycol) (PEG) chains whose terminal functional groups (A and B) are mutually reactive.

b Control parameters of network density of tetra gel. In the polymer network after completion of the chemical reaction, the molar mass of precursors M corresponds to the molecular weight between the cross-links ($M/2$), and the polymer concentration c represents the number density of cross-links n as $n = cN_A/M$. Here, N_A is the Avogadro constant.

II. PAST EXPERIMENTAL RESULTS OF LINEAR ELASTICITY IN TETRA GEL

In this section, we briefly review, in chronological order, our four experiments [15–18] that investigated the linear elasticity of polymer gels in the as-prepared state, using tetra gels (Fig. 1a). As shown in Fig. 1b, by tuning the molar mass M and concentration c of precursor solutions, we could independently and systematically control the network density, i.e., the molecular weight between the cross-links $M/2$ and the number density of the cross-links $n = cN_A/M$ in tetra gels. Here, N_A is the Avogadro constant, and c is defined as the precursor weight divided by the solvent volume, rather than by the solution volume (See Sec. S1 in Ref. [19]). In addition, we could control the network topology by tuning the following two parameters: (i) the connectivity p ($0 \leq p \leq 1$), i.e., the fraction of the reacted terminal functional groups to all the terminal functional groups;

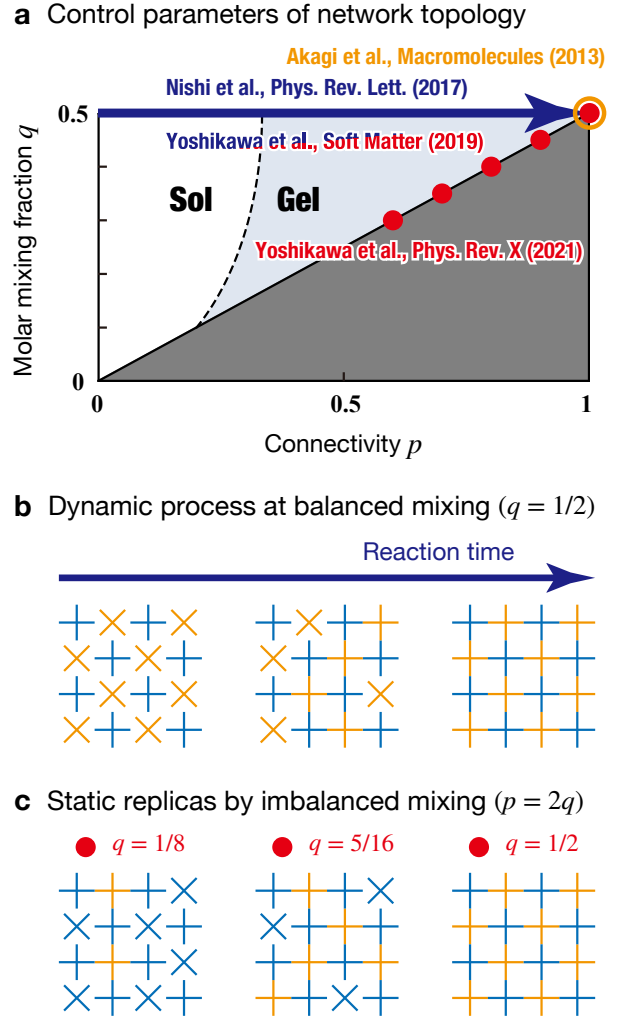


FIG. 2. **a** Control parameters of a network topology of tetra gel. The connectivity p increases monotonically with time and (ideally) reaches $p = 2q$ after completion of the reaction, where q is the molar mixing fraction of the precursors of the minor group.

b Dynamic process (DP) of gelation, where two precursors are mixed in a stoichiometrically balanced ratio ($q = 1/2$). **c** Static replicas (SR) of DP, where two precursors are mixed in a stoichiometrically imbalanced (and balanced) ratio ($0 \leq q \leq 1/2$). Here, the connectivity p after completion of the reaction is tuned as $p = 2q$.

and (ii) molar mixing fraction of minor precursors to all precursors q as $[A] : [B] = q : 1 - q$ ($0 \leq q \leq 1/2$). Each of these experiments [15–18] deals with different network topologies, and is summarized in Fig. 2a. Akagi et al. [15] investigated the network with $p \simeq 1$ (after completion of the reaction) and $q = 1/2$ (stoichiometrically balanced mixing), as shown by the orange circle in Fig. 2a. Nishi et al. [16] investigated the network with $q = 1/2$, as shown by the blue arrow in Fig. 2a and Fig. 2b. Yoshikawa et al. [17] compared the network with $q = 1/2$ (blue arrow in 2a and 2b) and $p = 2q$ (red

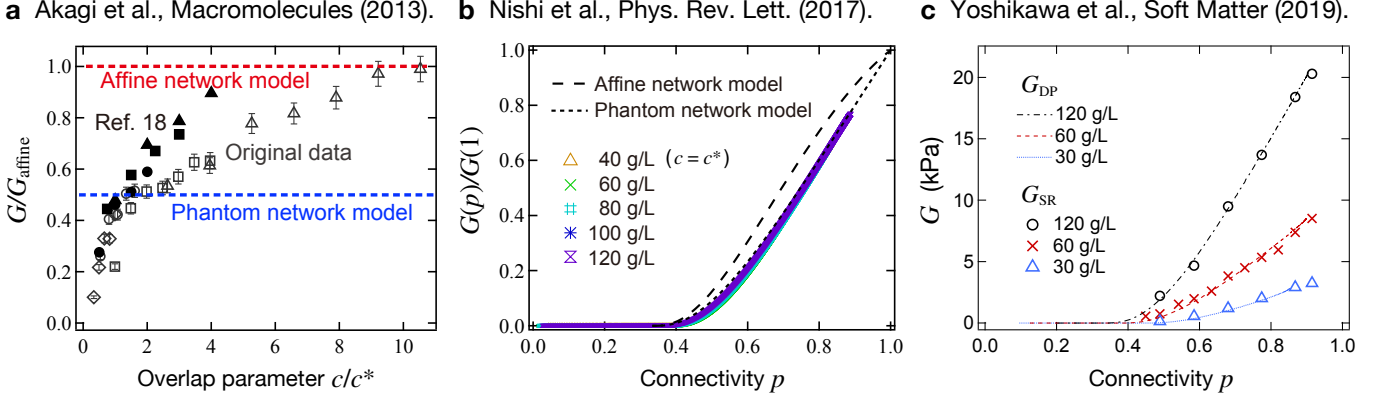


FIG. 3. Representative experimental results before the discovery of negative energy elasticity.

a Normalized shear modulus (G/G_{affine}) as a function of the overlap parameter (c/c^*). The open gray symbols represent the data from the original paper [15], which are inaccurate due to the samples and measurement method. The filled black symbols represent the data from Ref. [18] that are more accurate in terms of the samples and measurement method (see main text). Rhombuses, circles, squares, and triangles represent $M = 5, 10, 20$, and 40 kg/mol, respectively. The blue and red dashed lines show $G/G_{\text{affine}} = 0.5$ (the prediction of the phantom network model) and 1 (the prediction of the affine network model), respectively. The overlap parameter in the horizontal axis is converted from the polymer volume fraction ϕ/ϕ^* (in the original paper [15]) to concentration c/c^* .

b Normalized shear modulus ($G(p)/G(1)$) as a function of the connectivity of the polymer network (p). The polymer concentrations are $c = 40, 60, 80, 100$, and 120 g/L. The molar mass of precursors is $M = 20$ kg/mol, and the corresponding overlap concentration is 40 g/L. We calculate the dashed lines from the affine and phantom network models with the Bethe approximation. The data are taken from Ref. [16].

c Shear modulus (G) as a function of the connectivity of the polymer network (p) in the dynamic gelation process (DP) and the static replica (SR). The polymer concentrations are $c = 30, 60$, and 120 g/L, and the molar mass of precursors is $M = 20$ kg/mol. The data are taken from Ref. [17]. We note that the data in **b** and **c** were measured accurately in the same way as Ref. [18].

filled circle in Fig. 2a and Fig. 2c). Yoshikawa et al. [18] investigated the networks with $q = 1/2$ and $p = 2q$ (red filled circle in Fig. 2a and Fig. 2c). We describe the details of these studies in the following.

The first two studies (Akagi et al. [15] and Nishi et al. [16]) investigated the applicability of the classical rubber theories to polymer-gel elasticity. The representative models are the affine [7] and phantom [8] network models, which predict shear modulus G as

$$G_{\text{affine}} = \nu n k_B T \quad (1)$$

and

$$G_{\text{phantom}} = \xi n k_B T, \quad (2)$$

respectively. Here, n , k_B , and T are the number density of cross-links, Boltzmann constant, and absolute temperature, respectively. In Eqs. (1) and (2), $\xi \equiv \nu - \mu$ is the difference between the number per precursor of the elastically effective chains (ν) and the cross-links (μ). We cannot experimentally observe ν and ξ . However, p and q can be observed and used to calculate the functions $\nu = \nu(p, q)$, $\mu = \mu(p, q)$, and $\xi = \xi(p, q)$ using the Bethe (i.e., tree) approximation [17, 20, 21]. The difference between these models (Eqs. (1) and (2)) is the way they deal with the fluctuation of cross-links.

The affine network model assumes that the cross-links are fixed to the gel and that the deformation of a chain follows a macroscopic deformation. On the other hand, the phantom network model assumes that the cross-links fluctuate and that the deformation of a chain is attenuated.

Akagi et al. [15] measured c and M dependences of the shear modulus G through stretching measurements of the network with $p \simeq 1$ and $q = 1/2$. (Strictly speaking, the connectivity p of all the completely reacted gel samples was almost constant, $p \simeq 0.9$.) Figure 3a demonstrates that all the data of the c/c^* dependence of G/G_{affine} with different M roughly collapse onto a single master curve. Here, c^* is the overlap concentration of precursors obtained by viscosity measurement. However, in the original paper [15], the measurement results (open gray symbols) were inaccurate for the following two reasons: (i) a lower elastic modulus than expected was observed because the tetra gels were prepared using precursors with the terminal functional groups (amine and N -hydroxysuccinimide) that undergo hydrolysis over time; (ii) the elastic modulus was measured by stretching measurement, which causes a large error. For an accurate discussion, Fig. 3a also shows the accurately remeasured data from Ref. [18] (filled black symbols), overcoming the above two problems; we (i)

used tetra gels prepared using the precursors with the terminal functional groups (maleimide and thiol) that do not cause hydrolysis, and (ii) measured their elastic modulus by dynamic rheological measurement. Here, the the normalization factors $c^* = c^*(M)$ are different; the original paper [15] uses $c^* = 120, 75, 40, 15$ g/L for $M = 5, 10, 20, 40$ kg/mol, respectively, whereas Ref. [18] uses $c^* = 60, 40, 30$ g/L for $M = 10, 20, 40$ kg/mol, respectively. We note that the following data (Figs. 3b and c below) were also accurately measured by the same way as Ref. [18].

Based on Fig. 3a, Akagi et al. misinterpreted (as inferred from our present understanding) that a crossover from the phantom network model to the affine network model occurs in polymer gels. In Fig. 3a, the horizontal line showing $G/G_{\text{affine}} = 0.5$ can be regarded as the prediction of the phantom network model, because

$$\frac{G_{\text{phantom}}}{G_{\text{affine}}} = \frac{\xi(p, 1/2)}{\nu(p, 1/2)} \simeq 0.5, \quad (3)$$

for a tetra-arm network at $p \simeq 1$. For $c \simeq c^*$, G agrees well with G_{phantom} , and for $c < c^*$, the values of G are smaller than that of G_{phantom} . This is probably due to an increase in ineffective connections for $c < c^*$ [17]. On the other hand, for $c > c^*$, G/G_{affine} increases to approach 1 as c increases. Previously, it was considered for conventional polymer gels that an increase of G/G_{affine} with an increase in c is due to the presence of trapped entanglements. However, the stress-elongation curve obeying the neo-Hookean model [22] and the fracture energy obeying the Lake-Thomas model [23] strongly suggest that this is not the case. Therefore, Akagi et al. interpreted that the result in Fig. 3a indicates a crossover from the phantom network model to the affine network model with an increase in c . However, this crossover is negated by the following p dependence results.

Nishi et al. [16] investigated p dependence of G in the range $c^* < c$ for a dynamic process (DP) in which a network is formed from two precursor solutions in a stoichiometric ratio ($q = 1/2$), as shown by the blue arrow in Fig. 2b. Just after mixing two precursor solutions, we measured the time (t) courses of (i) G by rheological measurements and (ii) p by ultraviolet-visible light spectroscopy. Combining $G = G(t)$ and $p = p(t)$, we had $G(p)$. Figure 3b shows $G(p)/G(1)$ as a function of p , where $G(1)$ is the extrapolation of $G(p)$ at $p = 1$ based on the percolated network model [24]. Figure 3b demonstrates that all the data of the p dependence of $G(p)/G(1)$ with different c (in the range of $c^* < c$) collapse onto a single master curve, corresponding to the prediction of the phantom network model under the Bethe approximation, $G_{\text{phantom}}(p)/G_{\text{phantom}}(1)$.

Yoshikawa et al. [17] compared two methodologies to measure the connectivity (p) dependence of shear

modulus G in AB-type polymerization. The first is to measure G during the dynamic process (DP) of gelation in a stoichiometric ratio ($q = 1/2$) as shown in Fig. 2b. The second is to measure G of samples whose p after completion of the reaction is tuned by mixing two precursors in a stoichiometrically imbalanced ($q < 1/2$) and balanced ($q = 1/2$) ratios. Here, assuming the complete reaction of a minor group, we have $p = 2q$. This methodology can be regarded as a static replica (SR) of DP as shown in Fig. 2c. In the former (DP), we obtain continuous p dependence by monitoring the time evolution of the same sample, whereas in the latter (SR), we obtain discrete p dependence by using different samples. The advantage of SR over DP is that it can accurately measure various physical properties of samples with different p over time because it is static. Figure 3c demonstrates that $G = G(p)$ in the two methodologies (DP and SR) agrees well in high p (i.e., $p > 0.75$). [In the low- p regime, close to the gelation point, the differences in the structural parameters become more pronounced, reflecting the differences in the topology of DP (e.g., $\xi(p, 1/2)$) and SR (e.g., $\xi(p, p/2)$). See Fig. 4 in Ref. [17].] Note that these behaviors of p -dependence of G in DP and SR are well reproduced by the phantom network model under the Bethe approximation.

The above series of researches [15–17] are based on the long-standing basic assumption that the polymer-gel elasticity is mainly determined by entropy contribution. Under this assumption, the polymer-gel elasticity has been discussed with the classical rubber elasticity theories [7–9] that predict that the shear modulus is proportional to the absolute temperature ($G \simeq aT$) such as Eqs. (1) and (2). As shown in Fig. 4a, many experimental studies on natural and synthetic rubbers [25–28] have confirmed $G \simeq aT$, which means G is mainly determined by entropy contribution. However, in the case of a polymer gel, the results analyzed using such an assumption ($G \simeq aT$) were found to be inconsistent, even for measurements of G at certain temperatures (room temperature). For example, these results shown in Figs. 3b and c seem to be inconsistent with the result of Fig. 3a; while Fig. 3a shows the crossover between the phantom and affine network models depending on c , Figs. 3b and c show good agreement with the phantom network model not depending on c . We cannot resolve this inconsistency as long as we assume $G \simeq aT$.

Yoshikawa et al. [18] examined whether the premise of $G \simeq aT$ [e.g., Eqs. (1) and (2)] holds for polymer gels by measuring the temperature (T) dependence of the shear modulus G . Taking advantage of SR, we prepared various gel samples with different network densities (various M and c) and network topologies (various p). As shown in Fig. 4b, we have found that $G = aT + b$ with a significant negative value b , contrary to the premise of the classical rubber elasticity theories. As we explain in the next section, the first and second terms (aT and b) correspond

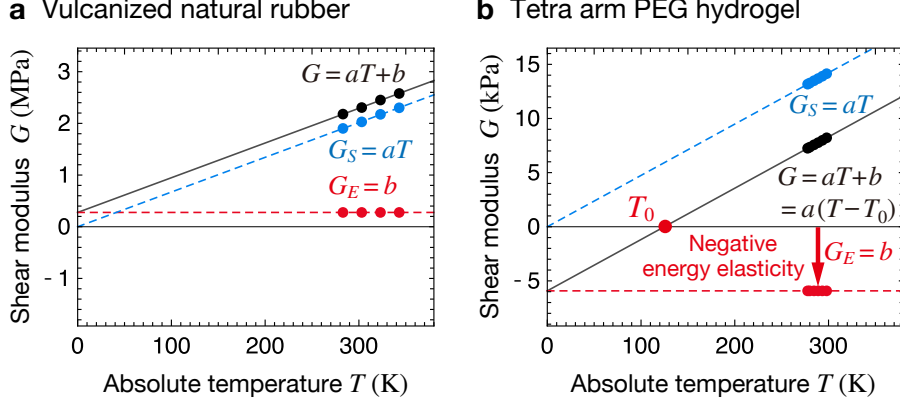


FIG. 4. **a-b** Decomposition of entropy and energy contributions to shear modulus in (a) vulcanized natural rubber and (b) tetra gel. We obtain the gray solid line from a least-squares fit to the temperature dependence of the shear modulus G (black symbols). According to Eq. (8), we have the entropy contribution G_S (blue dashed line) and the energy contribution G_E (red dashed line), which corresponds to the intercept of the gray solid line. The data are taken from Refs. [26] and [18] for **a** and **b**, respectively. Notably, the shear modulus of vulcanized natural rubber is proportional to the absolute temperature ($G \simeq aT$), while that of tetra gel is a linear function with a negative intercept [$G = a(T - T_0)$]. Here, the sample of tetra gel is synthesized by equal-weight mixing of the two kinds of precursors whose molar mass M and concentration c are 20 kg/mol and 60 g/L, respectively.

to entropy and internal energy contributions to G , respectively. Thus, the negative value of b is interpreted as “negative energy elasticity”. In Ref. [18], we confirm the above conclusions with more than 50 different network topologies and densities (Fig. 5). In the next section, we explain the negative energy elasticity based on thermodynamics and provide a self-contained description of the unified formula, which can explain all the experimental results of linear elasticity of PEG hydrogels with various network topologies and densities [15–18].

III. UNIFIED FORMULA FOR LINEAR ELASTICITY OF POLYMER GELS

This section provides a self-contained summary of the state-of-the-art understanding of the elasticity of isotropic, incompressible gels in the as-prepared state, as obtained using tetra gels with a homogenous network. In general, for homogeneous isotropic linear elastic materials, the elastic properties are uniquely determined by shear modulus G , i.e., any of the other elastic moduli can be calculated from G . For example, Young’s modulus E can be calculated as $E = 3G$, and the bulk modulus K is considered infinite ($K \gg G$). Therefore, the elasticity of polymer gels in the as-prepared state is entirely determined by G .

We consider the thermodynamics of the deformation of polymer gels in the as-prepared state. The derivative of the Helmholtz free energy F of an elastic body with an applied shear strain γ is given by $dF = -SdT - PdV + V\sigma d\gamma$ at temperature T and external pressure P [7, 29]. Here, S , V , and σ are the entropy, volume, and shear

stress, respectively. Polymer gels are considered to be incompressible, i.e., the relative volume change $\Delta V/V$ is negligible because the bulk modulus (of the order of GPa) is significantly larger than the shear modulus (of the order of kPa). (Detailed analysis of $\Delta V/V$ is given in Appendices B and C in Ref. [18].) Thus, we have

$$df = -sdT + \sigma d\gamma, \quad (4)$$

where $f \equiv F/V$ and $s \equiv S/V$ are the Helmholtz free energy and entropy densities, respectively.

In polymer physics, f of a polymer gel is often written in the form of two separate contributions as [7]

$$f(T, \gamma) = f_{\text{mix}}(T) + f_{\text{el}}(T, \gamma), \quad (5)$$

where $f_{\text{mix}}(T) \equiv f(T, 0)$ and $f_{\text{el}}(T, \gamma) \equiv f(T, \gamma) - f_{\text{mix}}(T)$ are the mixing and elastic free energy densities, respectively. Here, f_{mix} is independent of the applied shear strain γ because the volume V does not change with deformation. We emphasize that Eq. (5) does not provide any new information in the as-prepared state; it merely defines f_{mix} and f_{el} . Equation (4) gives the shear stress as $\sigma(T, \gamma) = \partial f(T, \gamma) / \partial \gamma$ in an isothermal process. Thus, the shear modulus ($G(T) \equiv \lim_{\gamma \rightarrow 0} \partial \sigma(T, \gamma) / \partial \gamma$) is related to the free energy as

$$G(T) \equiv \lim_{\gamma \rightarrow 0} \frac{\partial^2 f}{\partial \gamma^2}(T, \gamma) = \lim_{\gamma \rightarrow 0} \frac{\partial^2 f_{\text{el}}}{\partial \gamma^2}(T, \gamma). \quad (6)$$

Equation (6) indicates that f_{mix} does not contribute to the shear modulus G .

Recently, we obtained the unified expression of the shear modulus of the tetra gels as a function of the mi-

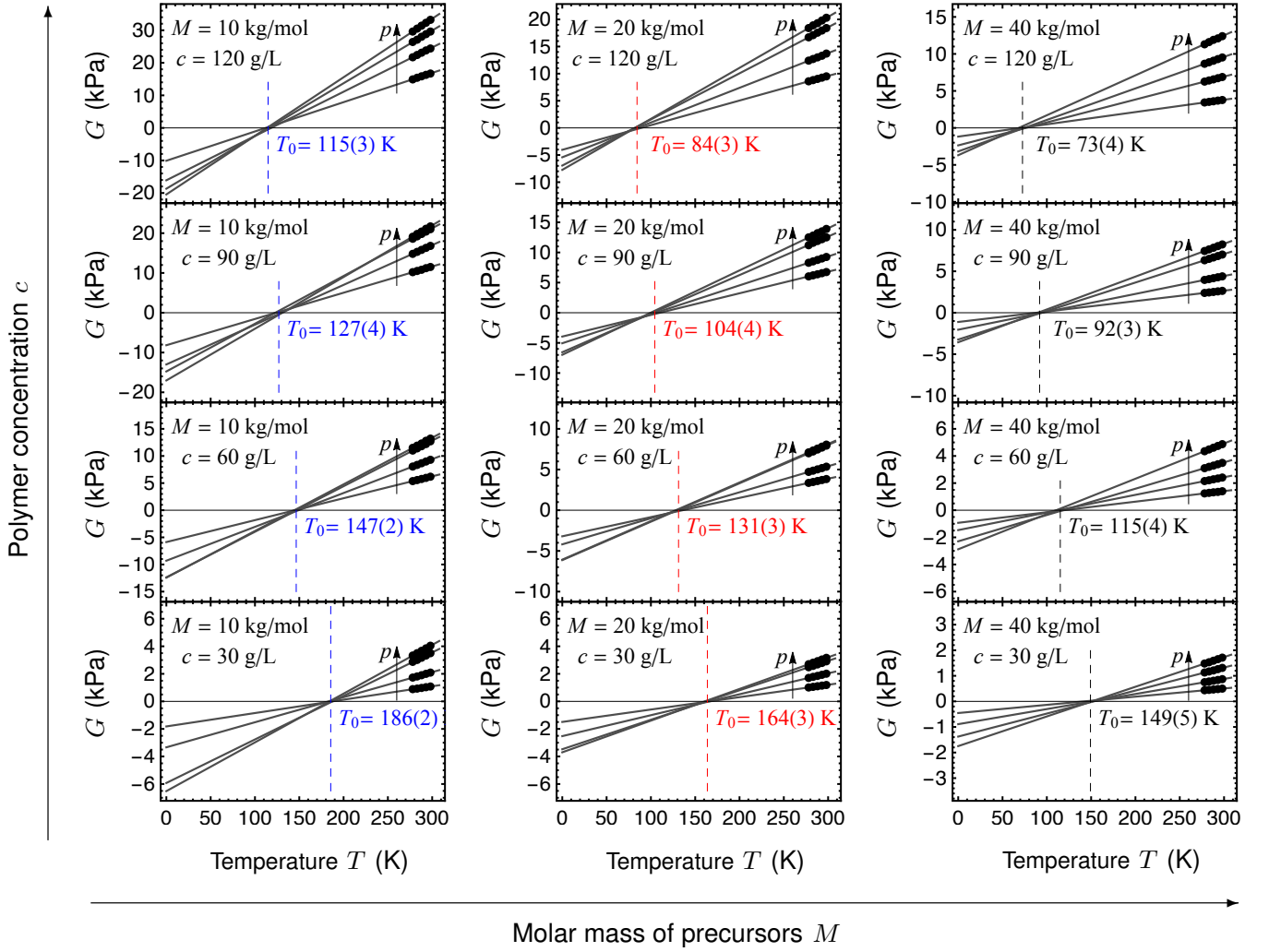


FIG. 5. Experimental evidence for the existence of negative energy elasticity in a polymer gel. All panels show the temperature (T) dependence of shear modulus G . We obtain each gray line from a least-square fit of each sample, which is characterized by the three parameters of the precursors: the molar mass M , the concentration c and the connectivity p . All gray lines that have the same M and c pass through a vanishing temperature T_0 on the T axis, which leads to Eq. (7). The value of T_0 in each graph is the average of the four samples with different values of p , and the values in parentheses represent the standard deviation. (Reprinted from Ref. [18]; CC BY 4.0).

crossoscopic structure of the polymer network as [18]

$$G(T; c, M, p, q) = a(c, M, p, q) \left[T - T_0 \left(\frac{c}{c^*(M)} \right) \right], \quad (7)$$

where c , M , p , and q are the polymer concentration, molecular weight of precursors, connectivity, and molar mixing fraction, respectively. (The definitions of p and q are given in the previous section.) Figures 5, 6a, and 6b experimentally validate Eq. (7) as follows. First, Fig. 5 shows that G is a nearly linear function of T [i.e., $G = aT + b = a(T - T_0)$, where $T_0 = -b/a$] in the measured range ($278 \text{ K} \leq T \leq 298 \text{ K}$). Second, Figs. 5 and 6a show that T_0 does not depend on the network topology (p and q), but depend on the network density (c and M). Finally, Fig. 6b demonstrates

that the dependence of c and M on T_0 is governed by $T_0 = T_0(c/c^*(M))$. Here, $c^*(M)$ is the normalization factor chosen to construct the master curve. We note that $c^*(M)$ is in close agreement with the overlap concentration of the precursors $c_{\text{vis}}^*(M)$ obtained by the viscosity measurement [15].

The first and second terms in Eq. (7) correspond to the entropy and energy elasticity, respectively. The Helmholtz free energy density satisfies $f = e - Ts$, where e is the internal energy density and s is the entropy density. Thus, on the basis of Eq. (6), we define the energy contribution G_E and the entropy contribution G_S to the shear modulus $G = G_E + G_S$ as $G_E \equiv \lim_{\gamma \rightarrow 0} (\partial^2 e / \partial \gamma^2)_{T,V}$ and $G_S \equiv$

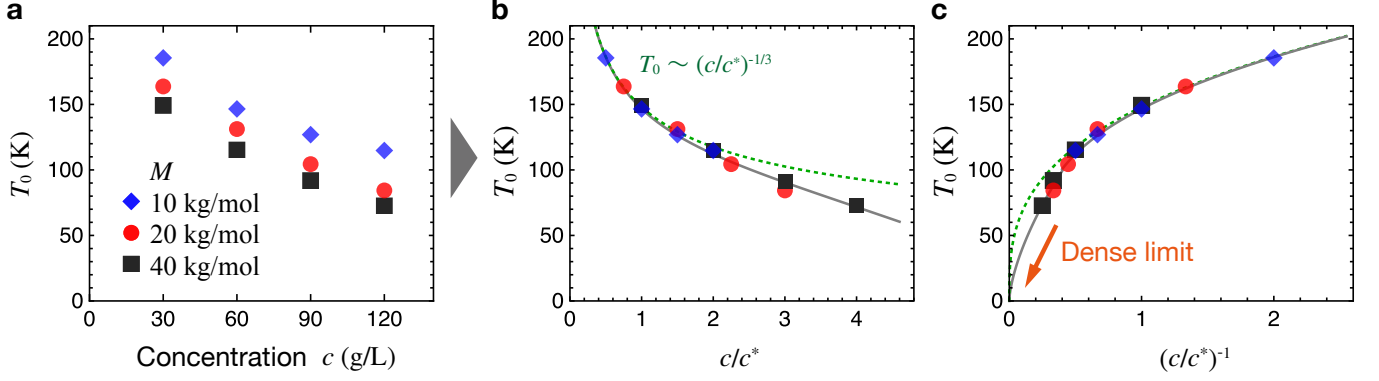


FIG. 6. **a** The concentration (c) dependence of the vanishing temperature T_0 that governs the energy contribution of polymer-gel elasticity. The blue diamonds, red circles, and black squares represent $M = 10, 20$, and 40 kg/mol, respectively. Each symbol represents the average of four samples taken from Fig. 5 (i.e., the data are taken from Ref. [18]). **b, c** The master curve of T_0 obtained by normalizing the concentration. Here, we set $c^* = 60, 40$, and 30 g/L for $M = 10, 20$, and 40 kg/mol, respectively. The green dashed curve shows the scaling law $T_0 \sim (c/c^*)^{-1/3}$ in the dilute regime ($c/c^* < 1$). As $(c/c^*)^{-1} \rightarrow 0$ (the dense limit), T_0 decreases, approaching nearly zero.

$-\lim_{\gamma \rightarrow 0} T (\partial^2 s / \partial \gamma^2)_{T,V}$, respectively. Here, G_S and G_E are defined under a constant-volume condition. According to the Maxwell relation $(\partial s / \partial \gamma)_{T,V} = -(\partial \sigma / \partial T)_{\gamma,V}$, we have

$$G_S(T) = T \frac{dG}{dT}(T), \quad (8)$$

which enables us to determine the entropy and energy contributions from the temperature (T) dependence of the shear modulus G under a constant-volume condition [7, 30, 31]. Substituting Eq. (7) into Eq. (8), we have $G_S = aT$ and $G_E = G - G_S = -aT_0$.

All measured samples shown in Fig. 5 have a significant negative G_E , which indicates that the undeformed state is unstable in terms of the internal energy. Because the (total) shear moduli of stable materials are generally bound to be positive ($G > 0$), $G_S = aT$ must be larger than $|G_E| = aT_0$.

We discuss Eq. (7) in the dilute, semidilute, and dense regimes, respectively. In the dilute regime ($c/c^*(M) < 1$), Fig. 6b demonstrates that the scaling law $T_0 \sim (c/c^*(M))^{-1/3}$, which would be a key to further understanding of the microscopic origin of negative energy elasticity in the future. We give a further discussion in Ref. [18].

In the semidilute regime ($1 \lesssim c/c^*(M) \lesssim 4$) and sufficiently high p (i.e., $p > 0.75$), our experiment [17, 18] shows that the entropy contribution G_S of the tetra gel is phenomenologically well reproduced by a constant multiple of the phantom network model [Eq. (2)] as $G_S \simeq 2.4G_{\text{phantom}} \equiv 2.4\xi n k_B T$, where $n = n(c, M) = cN_A/M$ is the number density of the tetra-arm precursors. This implies that the prefactor $a(c, M, p, q)$ is approximately

separable into the product of the network-density contribution (the control parameters are c and M , Fig. 1b) and the network-topology contribution (the control parameters are p and q , Fig. 2a) as

$$a(c, M, p, q) \simeq 2.4k_B n(c, M) \xi(p, q). \quad (9)$$

We note that Eq. (9) is valid in the semidilute regime ($1 \lesssim c/c^*(M) \lesssim 4$) and sufficiently high p . In fact, $a(c, M, p, q)$ is a complex function in the dilute regime ($c/c^*(M) < 1$) or low p [see Fig. 5(d) in Ref. [18]].

In the dense regime, Fig. 6c indicates that T_0 decreases, approaching nearly zero as $(c/c^*)^{-1} \rightarrow 0$, which means that the solvent is removed. This result is in agreement with experimental results on vulcanized natural rubber and synthetic rubbers without solvent; the absolute value of G_E is much smaller than the value of G_S [25, 27, 28]. In other words, this result suggests that the negative energy elasticity in the polymer gels originates from a solvent.

IV. RE-EXAMINATION OF PAST EXPERIMENTAL RESULTS BY UNIFIED FORMULA

Based on the unified formula in Eq. (7) together with the phenomenological expression of prefactor in Eq. (9), we re-examine past experimental results on polymer-gel elasticity [15–17]. First, we consider Akagi et al. [15], who investigated the network with $p \simeq 1$ and $q = 1/2$, as shown by the orange circle in Fig. 2a. Substituting

Eq. (9) into Eq. (7) and using Eq. (1), we have

$$\begin{aligned} \frac{G(T; c, M, 1, \frac{1}{2})}{G_{\text{affine}}(T; c, M, 1, \frac{1}{2})} &\simeq \frac{2.4\xi(1, \frac{1}{2}) \left[T - T_0 \left(\frac{c}{c^*(M)} \right) \right]}{\nu(1, \frac{1}{2}) T} \\ &\simeq 1.2 \left[1 - \frac{T_0 \left(\frac{c}{c^*(M)} \right)}{T} \right]. \end{aligned} \quad (10)$$

Here, we use $\xi(1, 1/2) = 1$ and $\nu(1, 1/2) = 2$. Equation (10) shows that G/G_{affine} depends only on c/c^* at isothermal conditions (i.e., T is constant), which elucidates Fig. 3a. We emphasize that “the crossover” in Fig. 3a does not mean the phantom-affine crossover, but originates from the concentration dependence of the negative energy elasticity (i.e., the dependence of T_0 on c/c^*).

Second, we consider the findings of Nishi et al. [16] on the network with $q = 1/2$, as shown by the blue arrow in Fig. 2a. In Fig. 3b, Nishi et al. [16] considered $G(p)/G(1)$, i.e., the shear modulus $G(p)$ normalized by the modulus of the network with $p = 1$ and $q = 1/2$. To generalize this, we consider $G(p, q)/G(1, 1/2)$, i.e., the shear modulus $G(p, q)$ with general q normalized by the modulus of the network with $p = 1$ and $q = 1/2$. Substituting Eq. (9) into Eq. (7), we have

$$\frac{G(T; c, M, p, q)}{G(T; c, M, 1, 1/2)} = \frac{a(c, M, p, q)}{a(c, M, 1, 1/2)} \simeq \xi(p, q). \quad (11)$$

Equation (11) (with $q = 1/2$) fully explains the result of Fig. 3b. The ratio $G(T; c, M, p, q)/G(T; c, M, 1, 1/2)$ does not depend on T , c , and M , and explained by $\xi(p, q)$, corresponding to the prediction of the phantom network model under the Bethe approximation. In the previous section, we mentioned that the results of Akagi et al. [15] and Nishi et al. [16] seem to be inconsistent with each other. However, the unified formula [Eq. (7) with Eq. (9)] can explain both in a consistent manner.

Third, we consider Yoshikawa et al. [17] that compared the networks with $q = 1/2$ (blue arrow in Fig. 2a) and $p = 2q$ (red filled circle in Fig. 2a). The former is a dynamic process (DP) as shown in Fig. 2b, and the latter is a static replica (SR) as shown in Fig. 2c. [In Ref. [17], we referred to SR as imbalanced mixing (IM).] From the unified formula [Eq. (7) with Eq. (9)], we derive that the connectivity (p) dependence of the shear modulus of DP ($G_{\text{DP}}(p)$) and that of SR ($G_{\text{SR}}(p)$) agree well in high p (i.e., $p > 0.75$), as shown in Fig. 3c. Because $G_{\text{DP}}(p) \equiv G(T; c, M, p, 1/2)$ and $G_{\text{SR}}(p) \equiv G(T; c, M, p, p/2)$, we obtain

$$\frac{G_{\text{SR}}(p)}{G_{\text{DP}}(p)} \simeq \frac{\xi_{\text{SR}}(p)}{\xi_{\text{DP}}(p)}, \quad (12)$$

where

$$\xi_{\text{DP}}(p) \equiv \xi(p, 1/2) = 2p - 1 + O((1-p)^2) \quad (13)$$

$$\xi_{\text{SR}}(p) \equiv \xi(p, p/2) = 2p - 1 + O((1-p)^2). \quad (14)$$

Here, we use the Bethe approximation [17]. From Eqs. (12), (13), and (14), we have $G_{\text{DP}}(p) \simeq G_{\text{SR}}(p)$ for $p \simeq 1$. The essence of this result relies on the fact that the prefactor $a(c, M, p, q)$ is separable as in Eq. (9), which leads to

$$\frac{G(T; c, M, p, q)}{\xi(p, q)} \simeq 2.4k_B n(c, M) \left[T - T_0 \left(\frac{c}{c^*(M)} \right) \right]. \quad (15)$$

Thus, G/ξ is independent of network topology (p and q). In fact, Yoshikawa et al. [17] experimentally demonstrated that $G_{\text{DP}}(p)/\xi_{\text{DP}}(p) = G_{\text{SR}}(p)/\xi_{\text{SR}}(p)$ holds and $G_{\text{DP}}(p)/\xi_{\text{DP}}(p)$ (and $G_{\text{SR}}(p)/\xi_{\text{SR}}(p)$) does not depend on p in the semidilute ($1 \lesssim c/c^*(M) \lesssim 4$) and sufficiently high p regime.

V. SUMMARY AND FUTURE PROSPECTS

In this article, we have described how past experimental results [15–17] on the linear elasticity of polymer gels can be successfully explained by considering negative energy elasticity coexisting with entropy elasticity [18]. First, we have reviewed the experimental research [15–18] on the linear elasticity of polymer gel in the as-prepared state, using tetra gels. Each of these experiments deals with a different network topology (Fig. 2a). Figure 3 has shown representative experimental results. Second, we have provided the unified formula in Eq. (7) for the linear elasticity of polymer gels, which have been revealed in a series of studies [15–18]. In addition, in the semidilute ($1 \lesssim c/c^*(M) \lesssim 4$) and sufficiently high p regime, the prefactor $a(c, M, p, q)$ is separable as in Eq. (9). Finally, using this unified formula (7) together with the phenomenological expression of prefactor in Eq. (9), we explain the past experimental results [15–17] and resolve the past results that seem to be inconsistent with each other [15, 16].

The discovery of negative energy elasticity [18] is one of the most significant recent advances in the field of linear elasticity of polymer gels. The negative energy elasticity, which vanishes when the solvent is removed, is the critical factor that differentiates gels from rubbers. The models of classical rubber elasticity theories (such as the affine, phantom, and junction affine network models) are inapplicable to polymer gels; a relative change in shear modulus due to changes in temperature is several times greater than predicted by these models. Thus, the negative energy elasticity is of great practical importance because polymer gels are used at various temperatures.

The elucidation of the governing law of the shear modulus is expected to improve our understanding of the static and dynamic properties of swelling of polymer gels in solvents. This is because the swelling pressure (Π_{tot}) is determined by its shear modulus and osmotic pressure as $\Pi_{\text{tot}} = \Pi_{\text{mix}} + \Pi_{\text{el}}$, where Π_{mix} and Π_{el} are the solvent-polymer mixing (Π_{mix}) and elastic (Π_{el}) contributions, respectively. As an example of the static properties of swelling, we recently discovered the governing law of osmotic pressure throughout the gelation process involving both the sol and gel states [19]. Here, the osmotic pressure was obtained by controlling the swelling pressure of gels with an external solution and subtracting the elastic contribution (Π_{el}). As an example of the dynamic properties of swelling, we demonstrated a significant dependence of the elastic modulus on the collective diffusion coefficient of the polymer networks [32, 33]. Accordingly, elasticity is the basis of both static and dynamic properties of polymer gels, prompting us to revisit past previous studies.

A complete understanding of the linear elasticity of polymer gels is still elusive, and it is important to address the following three points. First, the microscopic origin of the negative energy elasticity needs to be clarified. In the Ref. [18], we inferred that the origin is the interaction between the polymer and the solvent. However, because we performed only macroscopic measurements [15–18], we need further investigations to clarify the microscopic origin. For example, molecular-scale experiments (such as light scattering and single-chain experiments [34, 35]) and numerical simulations (such as molecular dynamics simulations) will reveal the microscopic origin. A future theory that explains the origin of negative energy elasticity from the microscopic point of view should predict the vanishing temperature T_0 from the network structure. To construct such a theory, the scaling law $T_0 \sim (c/c^*(M))^{-1/3}$ in the dilute regime ($c/c^*(M) < 1$) in Fig. 6b would play a key role.

Second, in connection with the prefactor $a(c, M, p, q)$, we need to revisit the classical rubber elasticity theories, which are used to calculate the entropy elasticity of vari-

ous network models. Thus, it may be possible to explain entropy elasticity G_S by subtracting its energy elasticity G_E from the shear modulus G , i.e., $G_S = G - G_E$, rather than the elasticity itself (G). However, according to our experiments [18], G_S is 2.4 times higher than that of the phantom network model, as in Eq. (9). The universality and meaning of 2.4 is an important open question. For example, a recently proposed theory [36] that predicts G_S from the number of topological loop defects does not appear to explain our result because it predicts a lower G_S than that of the phantom network model.

Third, it is important to investigate whether our findings extend to other polymer gels as well: (i) homogeneous gels with other polymer-solvent systems, such as PEG-acetonitrile [37], poly(acrylic acid) (PAA)-water [38], poly(*N*-isopropylacrylamide) (PNIPA)-methanol [39], and poly(*n*-butyl acrylate) (PBA)-*N,N*-dimethylformamide (DMF) [40, 41] systems; (ii) gels with other network structures, such as near-critical gels [42] and topological gels [43]; (iii) gels synthesized by other types of polymerization, such as radical polymerization. We emphasize that G_S and G_E are defined (and Eq. (8) holds) under constant-volume conditions. Thus, it is necessary to confirm that the effect of volume changes due to temperature changes is negligible. It is difficult for a small group to experiment on all of these various polymer gels, and it is essential to investigate the linear elasticity by various groups.

ACKNOWLEDGMENTS

This work was supported by the Japan Society for the Promotion of Science (JSPS) through Grants-in-Aid for Early Career Scientists grant number 19K14672 to N.S, JSPS Fellows grant number 21J13478 to Y.Y, Scientific Research (B) grant number 18H02027 to T.S, Scientific Research (A) grant number 21H04688 to T.S, and Transformative Research Areas grant number 20H05733 to T.S. This work was also supported by the Japan Science and Technology Agency (JST) CREST grant number JPMJCR1992 to T.S.

-
- [1] Baziwane D, He Q. Gelatin: the paramount food additive. *Food Rev. Int.* **19**, 423–435 (2003).
 - [2] Saha D, Bhattacharya S. Hydrocolloids as thickening and gelling agents in food: a critical review. *J. Food Sci. Technol.* **47**, 587–597 (2010).
 - [3] Peng X, Guo S. Texture characteristics of soymilk gels formed by lactic fermentation: a comparison of soymilk prepared by blanching soybeans under different temperatures. *Food Hydrocoll.* **43**, 58–65 (2015).
 - [4] Yeo Y, Bellas E, Highley CB, Langer R, Kohane DS. Peritoneal adhesion prevention with an in situ cross-linkable hyaluronan gel containing tissue-type plasminogen activator in a rabbit repeated-injury model. *Biomaterials* **28**, 3704–3713 (2007).
 - [5] Gaharwar AK, Avery RK, Assmann A, Paul A, McKinley GH, Khademhosseini A, Olsen BD. Shear-thinning nano-composite hydrogels for the treatment of hemorrhage. *ACSNano* **8**, 9833–9842 (2014).
 - [6] Caló E, Khutoryanskiy VV. Biomedical applications of hydrogels: a review of patents and commercial products. *Eur. Polym. J.* **65**, 252–267 (2015).
 - [7] Flory P.J. Principles of polymer chemistry. (Cornell Uni-

- versity Press, Ithaca, 1953).
- [8] James HM, Guth E. Statistical thermodynamics of rubber elasticity. *J. Chem. Phys.* **21**, 1039–1049 (1953).
 - [9] Flory PJ. Theory of elasticity of polymer networks. The effect of local constraints on junctions. *J. Chem. Phys.* **66**, 5720–5729 (1977).
 - [10] Shibayama M. Spatial inhomogeneity and dynamic fluctuations of polymer gels. *Macromol. Chem. Phys.* **199**, 1–30 (1998).
 - [11] Hild G. Model networks based on ‘endlinking’ processes: synthesis, structure, and properties. *Prog. Polym. Sci.* **23**, 1019–1149 (1998).
 - [12] Patel SK, Malone S, Cohen C, Gillmor JR, Colby RH. Elastic modulus and equilibrium swelling of poly (dimethylsiloxane) networks. *Macromolecules* **25**, 5241–5251 (1992).
 - [13] Sakai T, Matsunaga T, Yamamoto Y, Ito C, Yoshida R, Suzuki S, *et al.* Design and fabrication of a high-strength hydrogel with ideally homogeneous network structure from tetrahedron-like macromonomers. *Macromolecules* **41**, 5379–5384 (2008).
 - [14] Matsunaga T, Sakai T, Akagi Y, Chung U, Shibayama M. SANS and SLS studies on tetra-arm PEG gels in as-prepared and swollen states. *Macromolecules* **42**, 6245–6252 (2009).
 - [15] Akagi Y, Gong JP, Chung U, Sakai T. Transition between phantom and affine network model observed in polymer gels with controlled network structure. *Macromolecules* **46**, 1035–1040 (2013).
 - [16] Nishi K, Fujii K, Chung U, Shibayama M, Sakai T. Experimental observation of two features unexpected from the classical theories of rubber elasticity. *Phys. Rev. Lett.* **119**, 267801 (2017).
 - [17] Yoshikawa Y, Sakumichi N, Chung U, Sakai T. Connectivity dependence of gelation and elasticity in AB-type polymerization: an experimental comparison of the dynamic process and stoichiometrically imbalanced mixing. *Soft Matter* **15**, 5017–5025 (2019).
 - [18] Yoshikawa Y, Sakumichi N, Chung U, Sakai T. Negative Energy Elasticity in a Rubberlike Gel. *Phys. Rev. X* **11**, 011045 (2021).
 - [19] Yasuda T, Sakumichi N, Chung U, Sakai T. Universal equation of state describes osmotic pressure throughout gelation process. *Phys. Rev. Lett.* **125**, 267801 (2020).
 - [20] Macosko CW, Miller DR. A new derivation of average molecular weights of nonlinear polymers. *Macromolecules* **9**, 199–206 (1976).
 - [21] Miller DR, Macosko CW. A new derivation of post gel properties of network polymers. *Macromolecules* **9**, 206–211 (1976).
 - [22] Sakai, T., Experimental verification of homogeneity in polymer gels. *Polym. J.* **46**, 517–523 (2014).
 - [23] Akagi Y, Sakurai H, Gong JP, Chung U, Sakai T. Fracture energy of polymer gels with controlled network structures. *J. Chem. Phys.* **139**, 144905 (2013).
 - [24] Nishi K, Noguchi H, Sakai T, Shibayama M. Rubber elasticity for percolation network consisting of Gaussian chains. *J. Chem. Phys.* **143**, 184905 (2015).
 - [25] Meyer KH and Ferri C. Sur l’élasticité du caoutchouc. *Helv. Chim. A.* **18**, 570–589 (1935).
 - [26] Anthony RL, Caston RH, and Guth E. Equations of state for natural and synthetic rubber-like materials. I. Unaccelerated natural soft rubber, *J. Phys. Chem.* **46**, 826 (1942).
 - [27] Mark JE and Flory PJ, Configuration of polyoxyethylene chain. *J. Am. Chem. Soc.* **87**, 1415–1423 (1965).
 - [28] Mark JE. Thermoelastic results on rubberlike networks and their bearing on the foundations of elasticity theory. *J. Polym. Sci. Macromol. Rev.* **11**, 135–159 (1976).
 - [29] Landau LD, Lifshitz EM. *Theory of Elasticity*. (Pergamon Press, Oxford, 1986).
 - [30] Fermi E. *Thermodynamics*. (Dover Publications, New York, 1937), Sec. 17.
 - [31] Rubinstein M, Colby RH. *Polymer physics*. (Oxford University Press, Oxford, 2003).
 - [32] Fujiyabu T, Yoshikawa Y, Kim J, Sakumichi N, Chung U, Sakai T. Shear modulus dependence of the diffusion coefficient of a polymer network. *Macromolecules* **52**, 9613–9619 (2019).
 - [33] Kim J, Fujiyabu T, Sakumichi N, Katashima T, Yoshikawa Y, Chung U, Sakai T. Mixing and elastic contributions to the diffusion coefficient of polymer networks. *Macromolecules* **53**, 7717–7725 (2020).
 - [34] Nakajima K, Watabe H, Nishi T. Single polymer chain rubber elasticity investigated by atomic force microscopy. *Polymer* **47**, 2505–2510 (2006).
 - [35] Liang X, Nakajima K. Nanofishing of a Single Polymer Chain: Temperature-Induced Coil-Globule Transition of Poly(N-isopropylacrylamide) Chain in Water. *Macromol. Chem. Phys.* **219**, 1700394 (2018).
 - [36] M. Zhong, R. Wang, K. Kawamoto, B. D. Olsen, J. A. Johnson, Quantifying the impact of molecular defects on polymer network elasticity. *Science* **353**, 1264–1268 (2016).
 - [37] Li X, Nakagawa S, Tsuji Y, Watanabe N, Shibayama M. Polymer gel with a flexible and highly ordered three-dimensional network synthesized via bond percolation. *Sci. Adv.* **5**, eaax8647 (2019).
 - [38] Oshima K, Fujimoto T, Minami E, Mitsukami Y. Model Polyelectrolyte gels synthesized by end-linking of tetra-arm polymers with click chemistry: synthesis and mechanical properties. *Macromolecules* **47**, 7573–7580 (2014).
 - [39] Okaya Y, Jochi Y, Seki T, Satoh K, Kamigaito M, Hoshino T, *et al.* Precise synthesis of a homogeneous thermoresponsive polymer network composed of four-branched star polymers with a narrow molecular weight distribution. *Macromolecules* **53**, 374–386 (2020).
 - [40] Huang X, Nakagawa S, Li X, Shibayama M, Yoshie N. A simple and versatile method for the construction of nearly ideal polymer networks. *Angew. Chem. Int. Ed.* **59**, 9646–9652 (2020).
 - [41] Nakagawa S, Yoshie N. Synthesis of a bottlebrush polymer gel with a uniform and controlled network structure. *ACS Macro Lett.* **10**, 186–191 (2021).
 - [42] Aoyama T, Yamada N, Urayama K. Nonlinear Elasticity of Ultrasoft Near-Critical Gels with Extremely Sparse Network Structures Revealed by Biaxial Stretching. *Macromolecules* (2021).
 - [43] Ito K. Novel cross-linking concept of Polymer Network: synthesis, structure, and properties of slide-ring gels with freely movable junctions. *Polym. J.* **39**, 489–499 (2007).